ELSEVIER

Biochimica et Biophysica Acta 1506 (2001) 260–267

BIOCHIMICA ET BIOPHYSICA ACTA
BBA

www.bba-direct.com

Evaluation of the energetic position of the lowest excited singlet state of β-carotene by NEXAFS and photoemission spectroscopy

M. Beck *, H. Stiel, D. Leupold, B. Winter, D. Pop, U. Vogt, C. Spitz [1]

Max-Born-Institut für Nichtlineare Optik und Kurzzeitspektroskopie, Max-Born-Str. 2A, D-12489 Berlin, Germany

Received 19 July 2001; received in revised form 18 October 2001; accepted 19 October 2001

Abstract

In carotenoids the lowest energetic optical transition belonging to the π-electron system is forbidden by symmetry, therefore the energetic position of the S_1 (2^1A_g) level can hardly be assessed by optical spectroscopy. We introduce a novel experimental approach: For molecules with π-electron systems the transition C1s → 2p(π*) from inner-atomic to the lowest unoccupied molecular orbital (LUMO) appears in X-ray absorption near edge spectra (NEXAFS) as an intense, sharp peak a few eV below the carbon K-edge. Whereas the peak position reflects the energy of the first excited singlet state in relation to the ionization potential of the molecule, intensity and width of the transition depend on hybridization and bonding partners of the selected atom. Complementary information can be obtained from ultraviolet photoelectron spectroscopy (UPS): At the low binding energy site of the spectrum a peak related to the highest occupied molecular orbital (HOMO) appears. We have measured NEXAFS and UPS of β-carotene. Based on these measurements and quantum chemical calculations the HOMO and LUMO energies can be derived.

Keywords: NEXAFS; UPS; β-carotene; HOMO; LUMO; S_1

1. Introduction

Carotenoids (and their oxygen-containing derivatives, the xanthophylls) are essential components of pigment protein complexes (most 'antennae' and all reaction centers) in photosynthetic organisms. β-Carotenes which our measurements are concentrated on are located in core antenna complexes CP43 and CP47 of the photosystem II [1]. Carotenoids fulfill the three functions of (i) light harvesting (absorption and energy transfer), (ii) regulation of internal energy flow under external levels of sunlight varying over orders of magnitude in intensity and pigment protection against photobleaching and (iii) stabilization of the pigment protein network [2].

With respect to the former two tasks, the first excited singlet state S_1 (2^1A_g) is assumed to play a central role. For the antennae of higher plants it is hypothesized that both the energy transfer xanthophyll → chlorophyll (Chl) and a photoprotective transfer Chl → xanthophyll occur via this xanthophyll S_1 level [3]. Remarkably, for the carotenoids and xanthophylls of photosynthetic relevance the optical (one-photon) transition from the electronic ground state S_0 (1^1A_g) of the π-electron system to

* Corresponding author. Fax: +49-30-6392-1309.
E-mail address: beck@mbi-berlin.de (M. Beck).
[1] Present address: Universitaet Potsdam, Institut für Experimentalphysik, Photonik, Am neuen Plais 10, D-14469 Potsdam, Germany.

0005-2728/01/$ – see front matter
PII: S0005-2728(01)00226-2

the S_1 (2^1A_g) state is forbidden because they belong both to the same symmetry. There seems to be only one attempt in literature to measure directly the extremely weak one-photon transition to S_1 [4]. Instead, much attention has been devoted recently by other groups to elucidate the energetic position of S_1 by indirect spectroscopic methods like (i) two-photon excitation profile of excited state absorption [5], (ii) two-photon excitation profile of Chl fluorescence [6], (iii) excitation profiles of resonance Raman spectra [7]. There are also attempts to measure the very weak S_1 fluorescence [8]. Until now the results obtained this way are valid only for dissolved xanthophylls or/and are contradictory (cf. [9] for recent review). Moreover, a most recent re-evaluation of method (ii) has shown that in the spectral region of the expected two-photon transition to carotenoids S_1 there is effective two-photon absorption of Chl itself (M. Krikounova et al., unpublished data). Therefore utmost caution is advised in interpretation of experimental results achieved with method (ii). Therefore we are developing an alternative access to this intricate problem, based on pulsed near edge X-ray absorption spectroscopy (NEXAFS) at the carbon K-edge in synchronized combination with a suitable optical pump pulse tuned to the carotenoid/xanthophyll $S_0 \rightarrow S_2$ transition [10].

In the carbon NEXAFS spectrum of a pigment protein complex the transition from the carbon inner-atomic shell 1s to the lowest excited state of the molecular π-electron system of the carotenoids occurs as absorption band a few eV below the absorption profile of the K-edge, which may be overlapped by 1s-originated transitions in other carbons not belonging to the carotenoid. This latter problem can be minimized by selective marking of the carotenoid transition with a suitable pump pulse. Action of this pulse results in population changes in HOMO, LUMO+1, as well as, after fast relaxation, in LUMO, therefore an informative NEXAFS differential spectrum can be expected.

Here, as a first step towards determination of the energetic position of S_1 with respect to S_0 in carotenoids in photosynthetic antennae, we report on NEXAFS measurements of pure β-carotene deposited on thin Si_3N_4 foils, i.e. there are no other carbons in the sample. The NEXAFS-based determination of the energetic position of the LUMO is combined with determination of the HOMO position of the same samples by ultraviolet photoelectron spectroscopy (UPS). Both values are related to the ionization potential (IP, vacuum level), i.e. their difference is the result of interest, the energy of the transition $1^1A_g \rightarrow 2^1A_g$.

2. Materials and methods

2.1. Preparation of β-carotene samples

In preparation of the samples it was intended to get amorphous films of pure β-carotene. Crystallization was unwanted to avoid intermolecular coupling of the electronic states. The β-carotene (Sigma C0126) was kept and always handled either under nitrogen atmosphere in darkness or in vacuum better than 5×10^{-4} mbar. Further purification from remaining solvents and other volatile contamination was done during the vacuum sublimation procedure by carefully raising the temperature of the β-carotene powder in a quartz oven at pressures lower than 5×10^{-8} mbar.

Prior to the final preparation, for determining the optimum evaporation conditions (avoiding the appearance of decomposition molecular fragments formed during the heating process), studies using the quadrupole mass spectrometer were effected. Between 120°C and 170°C escaping benzene and a broad variety of other molecules was found in the mass spectrum below 400 AMU for a certain time. Beginning from 150°C a deposition could be determined on the microbalance as shown in Fig. 1a. Between 170°C and 190°C the emission of intact β-carotene could be identified in the mass spectrometer by the dominant mass peak at 536.6 AMU accompanied by some fragments built in the ionization procedure as shown in Fig. 1b. When raising the temperature above approximately 194°C β-carotene was irreversibly decomposed and the fragments were found in the mass spectrum in many peaks beyond 200 AMU as indicated in Fig. 1c. In further preparations the deposition temperature was 180°C and was carefully controlled not to exceed 185°C in any part of the oven. Deposition on the substrate was started after the mass peaks between 200 AMU and 400 AMU vanished. The sublimation rate was normally around

10^{-9} g/(min cm^2) depending on the filling level of the evaporator.

In order to ensure that β-carotene stays intact during the deposition procedure, a film of 5.5×10^{-7} g/cm^2 (±10%) was sublimed on a gold substrate and 4.0 cm^2 (±2%) of this film was washed off with 4 ml (±5%) acetone. The UV-VIS absorption band of this solution around 450 nm was slightly broadened by 10% in respect to the spectrum of β-carotene measured as bought. The peak extinction was 0.11 cm^{-1} which is 80% of the expected value based on a molar extinction coefficient of ε_{max} = 134.300 M^{-1} cm^{-1} [11]. This loss of peak extinction stands in line with the observed broadening of the spectrum.

In order to judge the extent of crystallization in the film, β-carotene was sublimed onto quartz and sapphire substrates. The UV-VIS absorption spectra of the films on these substrates did not differ from each other and, as demonstrated in Fig. 2, clearly show the absorption band around 450 nm (2.75 eV), admittedly broadened in respect to the spectrum of β-carotene solution. In crystalline samples, because they easily result from drying a solution on a plane support, the absorption band around 450 nm has not been observed.

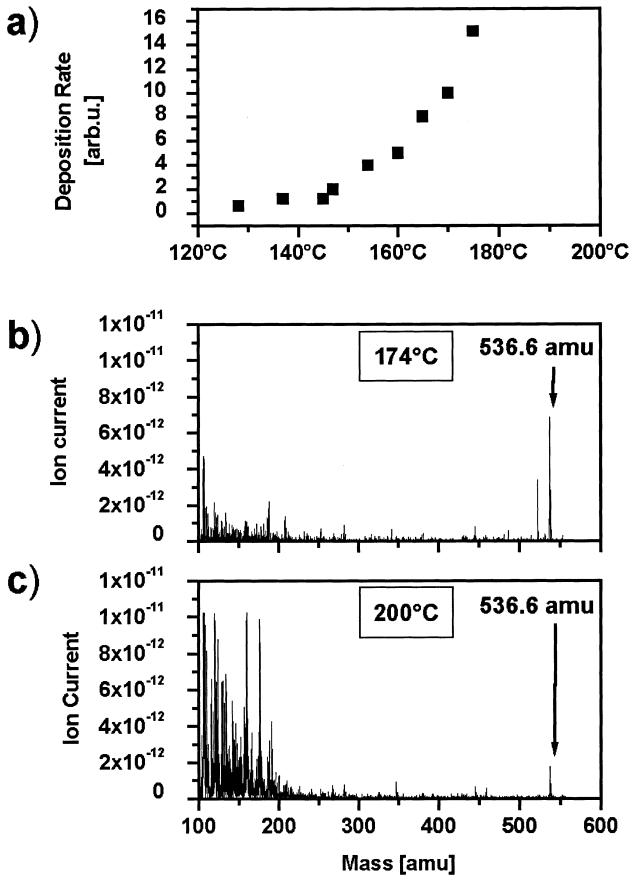

Fig. 1. Mass spectra of evaporated β-carotene. (a) Deposition rate at different temperatures. (b) Mass spectrum at 174°C. (c) Mass spectrum at 200°C. Note the same vertical scaling. The mass peak of β-carotene is indicated (536.6 AMU).

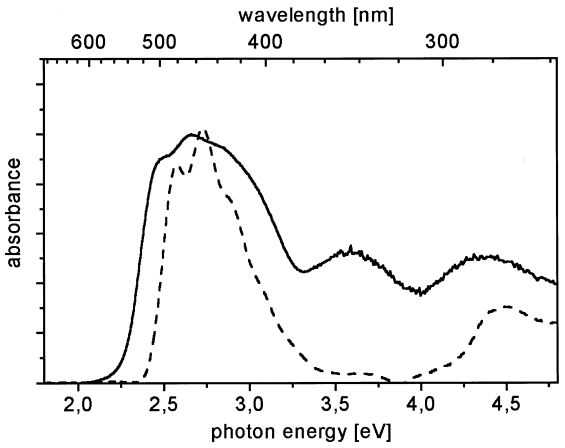

Fig. 2. UV/VIS absorption spectra of β-carotene sublimed as a film on sapphire (solid line) and dissolved in *n*-propanol (dashed line).

2.2. UPS

The experiment was performed in an ultrahigh vacuum system (base pressure 2×10^{-10} mbar) consisting of interconnected load-lock, preparation and analysis chambers and a manipulator for sample transfer and handling. The UHV apparatus is equipped with an OMICRON EA 125 hemispherical electron energy analyzer, a He-lamp, UHV evaporators, a quadrupole mass spectrometer and an Ar^+ sputter gun.

Immediately after deposition, the samples were transferred into the analysis chamber without breaking the UHV. Photoelectrons were detected by the hemispherical electron analyzer to within ±1° acceptance angle, normal to the surface and the signal was recorded by counting electronics. For the current experiments the pass energy of the analyzer was set to 10 eV, which corresponds to approximately 200 meV resolution. During measurements the sample was kept at ground potential, except in the cases when it was biased at −7 V for determining the low energy cut off of the spectra.

To perform UPS measurements the molecules were deposited as thin films on polycrystalline Au. The Au was cleaned by repeated cycles of Ar^+ sputtering (typical value for sample current approximately 6.7 mA) and annealing at 750°C. The β-carotene films were obtained by evaporating the materials from UHV evaporators at a temperature of 180°C and subliming on the Au at pressure below 5×10^{-8} mbar in a distance of 4 cm between oven and substrate.

In a first experiment charging of the β-carotene film was excluded. This was done as follows: β-carotene was sublimed in portions of 7.5×10^{-8} g/cm^2. For each film thickness an UPS spectrum was taken under He(I) ($h\nu=21.22$ eV) illumination. The rough surface of the gold substrate allowed in this case detection simultaneously of the electrons coming from gold and the electrons coming from the film up to a thickness of 1.5×10^{-7} g/cm^2. The difference of the 7.5×10^{-8} g/cm^2 film to the pure gold spectrum (scaled by the height of the Fermi edge) yields surprisingly well the spectrum of the 5.5×10^{-7} g/cm^2 film and, hence, charging of the β-carotene film can be excluded within an accuracy of 200 mV.

In a second experiment the gold substrate was cleaned as before and a 5×10^{-7} g/cm^2 film was sublimed in one step under the same conditions as above. The UPS spectrum was measured with 7 V bias and 10 eV pass energy. The bias voltage allows very accurately determination of the zero energy electrons. As electrostatic charging of the β-carotene film under UPS measurement can be excluded (see above), the binding energies of the electronic states may be determined knowing the zero energy cut off in the spectrum and the energy of He(I) photons.

2.3. NEXAFS

For NEXAFS measurements a laboratory X-ray absorption spectrometer based on a pulsed laser plasma source was utilized [12]. The experimental arrangement is shown in Fig. 3. The XUV source was a plasma on a copper target produced by a Nd:YAG laser (Brilliant, Quantel). The laser system operating at 10 Hz delivered pulses with pulse duration of 4 ns and a single pulse energy of about 180 mJ. The laser radiation ($\lambda=1.064$ nm) was focused by a plano-convex lens ($f=50$ mm) to a peak intensity of about 1×10^{14} W/cm^2. The resulting plasma emitted XUV radiation from an area with a diameter of about 25 μm. The intensity and stability of the XUV emission was controlled by a windowless photodiode (G1126-2, Hamamatsu) which was covered by a thin (200 nm) Al filter.

A transmission grating spectrograph similar to that described in [13] was used: A slit (width 50 μm) ahead of the grating projected an image of the X-ray source onto the detector, which was spectrally split up by the grating. The transmission grating, which was unsupported, had a grating constant of 100 nm with a line to space ratio of nearly 1:1 and was structured into a silicon foil. To enhance its diffraction efficiency the grating was evaporated with 30 nm gold. The distances source–grating and grating–CCD were 900 mm and 950 mm respectively. Thereby the relative spectral resolving power $\lambda/\Delta\lambda$ at the carbon K-edge ($E=285$ eV) amounts to about 270, corresponding to an energy resolution of about 1 eV.

The emission spectra were detected with a calibrated thinned, back illuminated slow scan CCD camera (Photometrics CH350; 512×512 pixel). A thin Al filter (thickness 200 nm) was placed in front of the slit before the grating to suppress scattered visible light. Both the slit grating spectrograph and the CCD camera were situated in a vacuum chamber at a pressure below 5×10^{-4} mbar.

To perform NEXAFS, β-carotene was deposited onto thin Si_3N_4 foils (100 nm thickness, Silson,

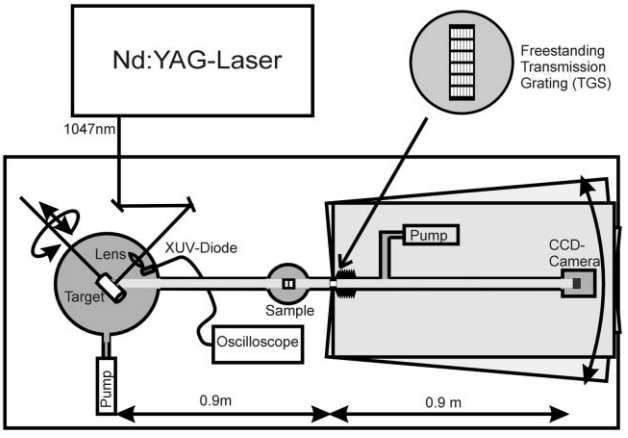

Fig. 3. Setup of the NEXAFS spectrograph (explanation see text).

Ltd., UK) under the same conditions as for the UPS measurements. The samples were kept in darkness and under nitrogen atmosphere during the transfer to the separated vacuum chamber housing. The sample was mounted on a motorized stage in a housing which was placed in front of the grating (cf. Fig. 3). The absorption spectra were determined by measuring the spectrum of the plasma emission with and without being absorbed by the sample. After that, the latter was divided by the former resulting in the NEXAFS spectrum (according the Lambert–Beer law). The wavelength axis of the spectrometer was calibrated by assigned copper emission lines [14] with an accuracy better than 100 meV.

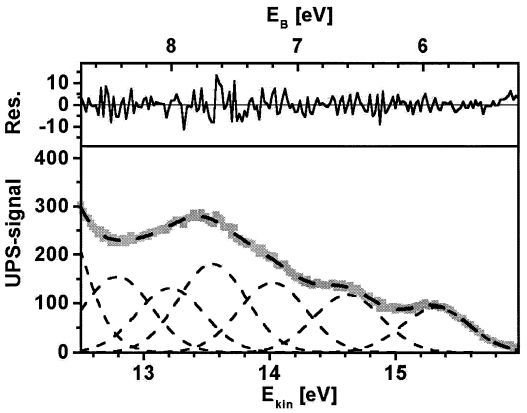

Fig. 5. UPS spectrum of β-carotene (gray dots) fitted by subbands (thin dashed lines). The resulting residuum is plotted above the spectrum comparing measurement and fit (thick dotted line).

3. Results

3.1. UPS spectra and simulation

In Fig. 4 the UPS photoelectron spectrum is shown as measured. The binding energy E_B relative to the vacuum level in this measurement could be scaled by use of the cut off value and the He(I) photon energy. As can be seen from Fig. 4 the UPS spectrum is well structured in the region of low binding energies. Furthermore the good signal to noise ratio in this region allows a deconvolution of the spectra. In order to reduce the number and range of parameters for this analysis molecular orbital (MO) calculations were carried out. The calculations were performed by GAUSSIAN 98 [15] using the Austin method 1 (AM1) [16], a semi-empirical method mainly used for ground state calculations of organic molecules. From optimizing the molecular structure the energies of the electronic states were evaluated. Rather than in the absolute values of the calculated energies, we were interested in the density of states near the band gap contributing to the photoelectron spectrum. Convolution of the highest occupied electronic states by Gaussian profiles (0.5 eV width) yields good agreement to the measured UPS spectra as shown in Fig. 4 neglecting a constant energy shift. Therefore we decided to deconvolute the measured spectra in the binding energy region between 5 and 9 eV by seven Gaussian profiles of equal width (starting value: 0.5 eV width) separated by equal distance representing the underlying six electronic states in this region, whereas the seventh curve stands for the rising continuum-like range. The results of this procedure together with the AM1 calculated binding energies are summarized in Fig. 5 and Table 1. As can be seen from the residues in Fig. 5 our model fits the experimental data very well. In comparison with AM1 calculations there is an energy shift between the calculated and the measured data. This constant energy shift can be attributed to environment polarization [17] that was not taken into account in our AM1 calculations. The calculated energy of the HOMO agrees very well with the gas phase ionization potential of 7.65 eV reported for

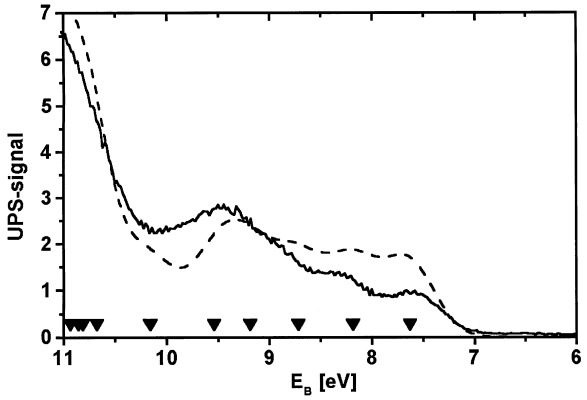

Fig. 4. Calculated energy levels (triangles) of β-carotene and the derived spectrum by convolution with a Gaussian profile of 0.5 eV FWHM (dashed line) in comparison with the measured UPS spectrum (solid line).

Table 1
Measured and calculated ionization energies of thin films of β-carotene on Au substrate

Energy (eV)	HOMO		HOMO-1		HOMO-2		HOMO-3		HOMO-4		HOMO-5
$E_{calculated}$	7.63		8.18		8.72		9.19		9.54		10.12
$E_{measured}$	5.84		6.56		7.12		7.56		7.94		8.48
ΔE (calc.)		0.55		0.53		0.47		0.35		0.58	
ΔE (meas.)		0.72		0.56		0.44		0.38		0.54	

Additionally energy differences $\Delta E = E(\text{HOMO-}n-1) - E(\text{HOMO-}n)$ are given. The calculated values were determined using GAUSSIAN/AM1. The experimental data were obtained from a deconvolution analysis of the UPS spectrum assuming seven Gaussian curves (cf. Fig. 5) where the seventh curve stands for the uprising continuum-like range. Error: ±0.2 eV.

β-carotene in [18]. The curve fitting yields a HOMO energy of the solid state β-carotene of 5.84 ± 0.2 eV giving a polarization energy of approximately 1.8 eV.

3.2. NEXAFS

The absorption spectrum of β-carotene near the carbon K-edge is shown in Fig. 6: The typical K-edge absorption structure of a single carbon atom is overlaid by a small preband at the low energy side and a more complex structure at higher energies. The latter structure belongs to the EXAFS range with high absorption cross-sections. At lower energies (below the ionization potential) the absorption cross-section drops and a narrow band with a shoulder appears. This second range was fitted by three Gaussian profiles as the spectral resolution is not enough to reveal the natural line shapes. The narrow band is positioned at 284.8 eV with an FWHM of 1.2 eV and the shoulder at 286.4 eV (FWHM 0.81 eV). The ascent of a broad band represents the carbon K-edge together with π* and σ* excitations (cf. [19]). We interpret the position of the third Gaussian profile at 288.8 eV as the ionization potential IP (in agreement with [19]). The narrow band is assigned to a transition $1s \rightarrow \pi^*$, where π* denotes an unoccupied molecular orbital. The observed peak represents a superposition of all (possibly chemically shifted) transitions from the carbon atoms in the polyene chain to this excited π* state. As no band is observed at lower energies we assign this band to the lowest unoccupied molecular orbital (LUMO). The shoulder seems to consist of only one line because its width gives $\lambda/\Delta\lambda = 350$, which is the value of the spectral resolution limit. But this is presently not certain because the width of the shoulder depends on the slope of the band representing the carbon K-edge. The natural linewidth of core-bound transitions can be estimated from the core hole life time via the Heisenberg uncertainty principle, which gives values below 0.1 eV for the carbon K-shell [20]. In agreement with

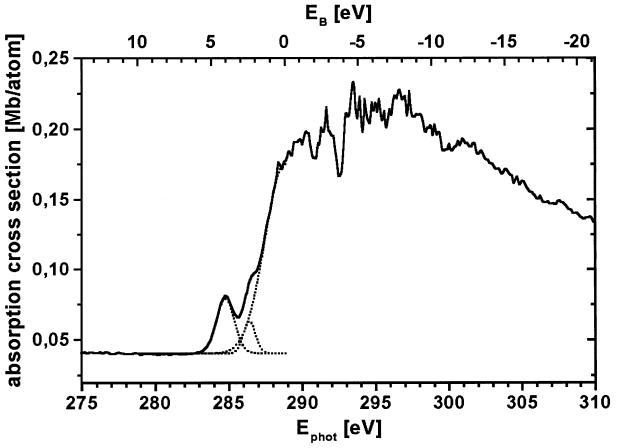

Fig. 6. NEXAFS spectrum of β-carotene (solid line). The dashed lines represent the fitted subbands below the ionization potential.

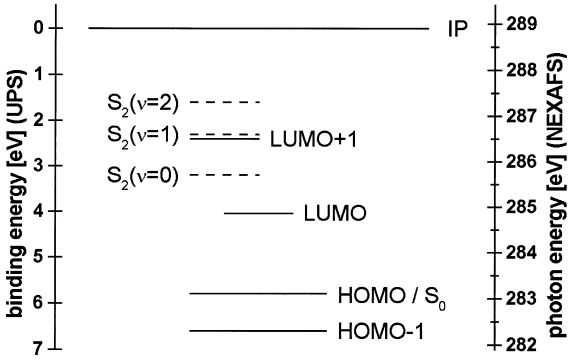

Fig. 7. Term scheme of amorphous β-carotene as resulting from NEXAFS (LUMO's) and UPS (HOMO's) (solid lines) as well as from the UV absorption spectrum (dashed lines). The UV absorption data are calculated by subtracting the energy of the absorption peaks (cf. Fig. 2) from the HOMO/S_0 level.

this high resolution measurements of electron energy spectra yielded for hydrocarbons linewidths of K-shell carbon electrons down to 0.1 eV [21]. The largest contribution to this shoulder could be assigned to the σ* (C–H) excitation which can be usually found around 287 eV for saturated hydrocarbons [22,23]. But we prefer the interpretation that this shoulder is caused by the π* (LUMO+1) level which should be found in this range or even lower (see Fig. 7). Into this level the electron from the HOMO gets excited by optical excitation as in UV/VIS spectroscopy (see Fig. 2). The alternative possibility of assignment does not affect much the considerations about the estimated value of the valence excitation energies because the K-shell ionization potential of a saturated hydrocarbon is typically around 290 eV [24]. This is almost the same value as the average value for the C atoms of the saturated chain.

Unfortunately the sample was relatively thick that the signal to noise ratio got worse in the higher energy range. This results in some artifacts. The two valleys at 292.5 eV and 290.9 eV can be assigned to lines of the copper emission being diffracted in the fourth order. These lines do not get absorbed by the aluminum filter. Therefore the fourth order of diffraction appears against the strongly absorbed first order of diffraction. As these lines above 1 keV are isolated there is no further disturbance of the spectrum, especially in the range around 285 eV. Interference by lower orders can be excluded as the aluminum filter absorbs in this range strongly.

4. Discussion

The MO energies of β-carotene evaluated by UPS and NEXAFS measurements together are summarized in an energy level scheme given in Fig. 7. For comparison the data from UV/VIS absorption measurements are also given. Using both the IP of 288.8 eV and the core energy of the lowest π* orbital of 284.8 eV as revealed from NEXAFS measurements the binding energy of the LUMO can be calculated to 4.0 ± 0.1 eV. The energy of the first excited singlet state S_1 of β-carotene can be estimated from the difference between this value and the HOMO energy (5.84 ± 0.20 eV) evaluated by UPS measurements. It amounts to 1.84 ± 0.20 eV which means the optically dark transition S_0–S_1 in amorphous β-carotene is located at about 650 nm. For comparison, values for the β-carotene S_0–S_1 transition in solution, obtained with the above-mentioned indirect methods, range between 540 nm and 735 nm [8,25–29]. No differences in the results between solid and dissolved β-carotene are expected as in the absorption spectra in the visible range no differences in the position of the bands were observed, only broadening (cf. Fig. 2). β-Carotene was examined in the same, solid phase in both UPS and NEXAFS measurements. So it can be expected that the differences in the electronic system are small, affected only by the different substrates.

To prove the reliability of the procedure described above we have compared the energy of higher excited singlet state(s) estimated from NEXAFS measurements with the related data from UV/VIS absorption spectra. From the position of the shoulder in the NEXAFS spectrum at 286.4 eV an energy of the higher excited singlet state S_x of 3.5 ± 0.2 eV was derived. As can be seen from Fig. 2 this value fits the position of the UV absorption band located at 3.7 eV very well.

Until now photoelectron spectra of carotenoids are known only for molecules in the gas phase [18] or from samples prepared under poorly defined conditions by evaporation of the solvent in vacuum [17]. An earlier X-ray photoelectron spectrum (XPS) of β-carotene excited utilizing Mg K_α radiation ($h\nu = 1253.6$ eV) can be found in [30]. Our HOMO energies are in good agreement with data published previously for the gas phase molecule [18] if we consider an energy shift of 1.8 eV caused by polarization effects (see above).

To our knowledge, the NEXAFS spectrum is the first one published of β-carotene. Near edge X-ray absorption fine structure (NEXAFS) spectroscopy is a well-established technique to study the electronic structure of unoccupied states of organic molecules with extended π-electron systems [31]. In this respect, a laboratory X-ray source offers some specific advantages in comparison with conventional X-ray sources such as easy access, compactness and short pulse length. We used our laser produced plasma XUV source together with our spectrograph to investigate NEXAFS spectra of β-carotene at the carbon K-edge.

A further improvement, of special interest for investigation of carotenoids in carbon-containing environment like light-harvesting complexes of higher plants or bacteria, should be possible with the pump-probe method, extending the setup described here. As can be seen from Fig. 6 the NEXAFS spectrum shows a spectral resolution high enough to discriminate energy levels separated by more than 1 eV. This will enable a pump-probe spectroscopy using a visible light pulse to excite the sample and to examine both occupied and unoccupied molecular states. Having the light sources for both the visible and the XUV range driven by the same laser, this setup will provide a jitter-free synchronization and thereby the feasibility of time-resolved NEXAFS investigations as described in [10,32]. Such investigations are currently in progress.

Acknowledgements

We thank T. Wilhein for providing us the transmission spectrograph and H. Lokstein for his valuable contributions in discussions. This work has been supported in part by the Deutsche Forschungsgemeinschaft (Le 729/2-3 and Ho 1757/2-2; SFB 429, TPA2).

References

[1] J. Shan, W. Jushuo, L. Li, N. Zhao, T. Kuang, Chin. Sci. Bull. 45 (2000) 1579–1583.
[2] H.A. Frank, R.J. Cogdell, Photochem. Photobiol. 63 (1996) 257–264.
[3] A.J. Young, D. Phillip, A.V. Ruban, P. Horton, H.A. Frank, Pure Appl. Chem. 69 (1997) 2125–2130.
[4] M. Mimuro, U. Nagashima, S.-i. Nagaoka, S. Takaichi, I. Yamazaki, Y. Nishimura, T. Katoh, Chem. Phys. Lett. 204 (1993) 101–105.
[5] P.J. Walla, P.A. Linden, G.R. Fleming, personal communication, 2000.
[6] P.J. Walla, J. Yom, B.P. Krueger, G.R. Fleming, J. Phys. Chem. B 104 (1999) 4799–4806.
[7] T. Sashima, M. Shiba, H. Hashimoto, H. Nagae, Y. Koyama, Chem. Phys. Lett. 290 (1998) 36–42.
[8] K. Onaka, R. Fujii, H. Nagae, M. Kuki, Y. Koyama, Y. Watanabe, Chem. Phys. Lett. 315 (1999) 75–81.
[9] H.A. Frank, Arch. Biochem. Biophys. 385 (2001) 53–60.
[10] H. Stiel, D. Leupold, M. Beck, I. Will, H. Lokstein, W. Sandner, J. Biochem. Biophys. Methods 48 (2001) 239–246.
[11] T. Hiyama, M. Nishimura, B. Chance, Anal. Biochem. 29 (1969) 339–350.
[12] M. Beck, U. Vogt, I. Will, A. Liero, H. Stiel, W. Sandner, T. Wilhein, Opt. Commun. 190 (2001) 317–326.
[13] T. Wilhein, S. Rehbein, D. Hambach, M. Berglund, L. Rymell, H.M. Hertz, Rev. Sci. Instrum. 70 (1999) 1694–1699.
[14] R.L. Kelly, http://cfa-www.harvard.edu/amdata/ampdata/kelly/kelly.html.
[15] M.J. Frisch, G.W. Trucks, H.B. Schlegel, G.E. Scuseria, M.A. Robb, J.R. Cheeseman, V.G. Zakrzewski, J.A. Montgomery, Jr., R.E. Stratmann, J.C. Burant, S. Dapprich, J.M. Millam, A.D. Daniels, K.N. Kudin, M.C. Strain, O. Farkas, J. Tomasi, V. Barone, M. Cossi, R. Cammi, B. Mennucci, C. Pomelli, C. Adamo, S. Clifford, J. Ochterski, G.A. Petersson, P.Y. Ayala, Q. Cui, K. Morokuma, D.K. Malick, A.D. Rabuck, K. Raghavachari, J.B. Foresman, J. Cioslowski, J.V. Ortiz, B.B. Stefanov, G. Liu, A. Liashenko, P. Piskorz, I. Komaromi, R. Gomperts, R.L. Martin, D.J. Fox, T. Keith, M.A. Al-Laham, C.Y. Peng, A. Nanayakkara, C. Gonzalez, M. Challacombe, P.M.W. Gill, B. Johnson, W. Chen, M.W. Wong, J.L. Andres, C. Gonzalez, M. Head-Gordon, E.S. Replogle, J.A. Pople, Revision A.5 edn., Gaussian, Inc., Pittsburgh, PA, 1998.
[16] M.J.S. Dewar, E.G. Zoebisch, E.F. Healy, J.J.P. Stewart, J. Am. Chem. Soc. 107 (1985) 3902–3909.
[17] F. Diepenbrock, P. Drusja, H.-D. Martin, K. Schaper, H.-H. Strehblow, J. Mol. Struct. 347 (1995) 429–438.
[18] D. Dougherty, E.S. Younathan, R. Voll, S. Abdulnur, S.P. McGlynn, J. Electron Spectrosc. Relat. Phenom. 13 (1978) 393–397.
[19] H. Carravetta, H. Agren, L.G.M. Pettersson, O. Vahtras, J. Chem. Phys. 102 (1995) 5589–5597.
[20] F. Brown, Solid State Phys. 29 (1974) 1–73.
[21] M. Tronc, G.C. King, F.H. Read, J. Phys. B 12 (1979) 137–157.
[22] A.P. Hitchcock, S. Beaulieu, T. Steel, J. Stöhr, F. Sette, J. Chem. Phys. 80 (1984) 3927–3935.
[23] A.P. Hitchcock, I. Ishii, J. Electron Spectrosc. Relat. Phenom. 42 (1987) 11–26.
[24] W.L. Jolly, K.D. Bomben, C.J. Eyermann, At. Data Nuclear Data Tables 31 (1984) 433–493.
[25] P.O. Andersson, S.M. Bachilo, R.L. Chen, T. Gillbro, J. Phys. Chem. 99 (1995) 16199–16209.
[26] S.L. Bondarev, V.N. Knyukshto, Chem. Phys. Lett. 225 (1994) 346–350.
[27] S.L. Bondarev, S.M. Bachilo, S.S. Dvornikov, S.A. Tikhomirov, J. Photochem. Photobiol. A 46 (1989) 315–322.
[28] V. Chynwat, H.A. Frank, Chem. Phys. 194 (1995) 237–244.
[29] R.J. Thrash, H.L.B. Fang, G.E. Leroi, J. Chem. Phys. 67 (1977) 5930–5933.
[30] N. Wada, T. Sagawa, J. Phys. Soc. Jpn. 43 (1977) 2107–2108.
[31] J. Stoehr, in: R. Gomer (Ed.), NEXAFS spectroscopy, Springer Series in Surface Sciences Vol. 25, 1; corrected printing edn., Springer, Berlin, 1992, pp. 403.
[32] Y. Iketaki, T. Watanabe, Opt. Eng. 35 (1996) 2418–2422.